Supporting Information

Conformation of Capping Ligands on Nanoplates: Facet-Edge-Induced Disorder and Self-Assembly-Related Ordering Revealed by Sum Frequency Generation Spectroscopy

Hao Zhang,[†,‡] *Fujin Li,*[†] *Qingbo Xiao,*[†] *Hongzhen Lin**[†]

[†]i-LAB, Suzhou Institute of Nano-Tech and Nano-Bionics (SINANO), Chinese Academy of Sciences, Suzhou 215123, P. R. China

[‡]School of Chemistry and Chemical Engineering, University of Chinese Academy of Sciences, 19A Yuquan Road, Beijing 100049, P.R. China

Contents:

1. SFG setup and sample preparation details

Our picosecond sum frequency generation (SFG) spectrometer laser system was built by EKSPLA, using a copropagating configuration. The visible signal at 532 nm and IR pulses around 2750-3000 cm^{-1} are about 25 ps at 50 Hz. The incident angle is 60° for the visible beam, and 55° for the IR beam. The energy of the visible and IR beams is generally less than 200 mJ and photodamage effect is negligible for the studied samples. The polarization combination is typically SSP during the experiment. To confirm the assignment of vibration modes and to estimate the methyl orientation angle, some samples are also measured with SPS and PPP polarizations.

The oleic acid-capped nanoplates were prepared according to the literature.[1-2] After being washed thoroughly to remove the free ligands, they were re-dispersed in chloroform to yield a stable stock solution. The concentration of the nanoplates was kept around 0.5 mg/mL. A certain volume of the stock solution was dropped onto water surface in a specially designed Teflon well, and the chloroform was allowed to evaporate at room temperature. The nanoplates are insoluble in water and most of them would be adsorbed to the water surface. Driven by surface tension and side-to-side attractions, the nanoplates tend to form 2D assemblies at sufficient coverage.[3] By tuning the added volume of the stock solution, the coverage rate of nanoplates on water surface was varied. The 2D arrangement and absence of face-to-face aggregation was confirmed using TEM. Control samples were also prepared by centrifuging the stock solution and drop-casting the supernatant onto water surface. It turns out that the interference from unbounded OA molecules and non-evaporable organic impurities, if any at all, is negligible and overwhelmed by the non-resonant background.

2. TEM images of nanoplates

Different amounts of $NaYF_4$ nanoplates were drop-cast on water surface and then gently transferred on to carbon-coated copper grids for TEM measurements. Evaporation of residue water inevitably promoted the assembly of the nanoplates to a greater extent in comparison to the situation on water surface. In a certain range of surface concentration, the nanoplates were well arranged in a 2D manner with little face-to-face overlapping. Size (side length of the hexagon top facet) distribution was derived based on the TEM images. The monodispersity of the nanoplates was not so good, but it does not affect the main observation and conclusion of this paper.

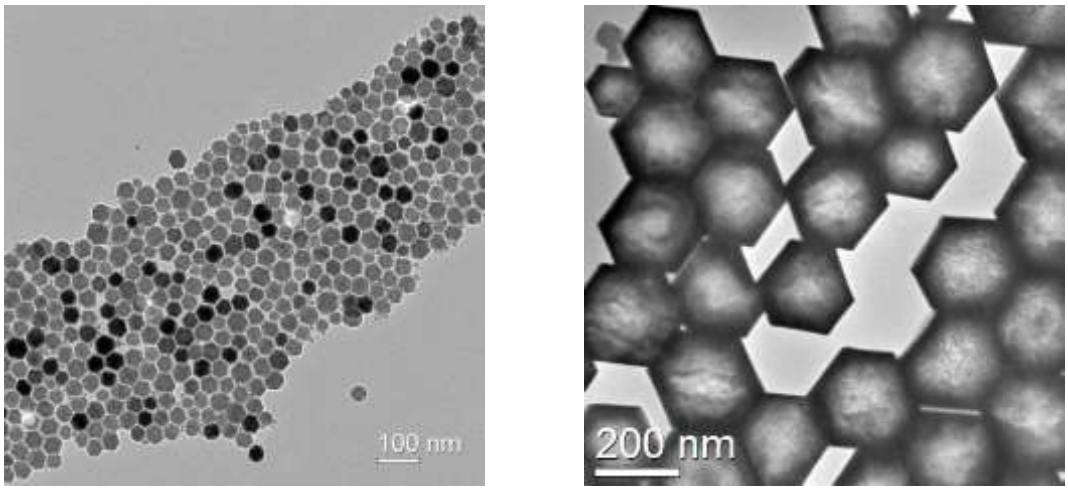

Figure S1. TEM images of hexagon $NaYF_4$ nanoplates with side lengths of 40±10 nm (left) and 140±40 nm (right).

3. Fitting parameters for the SFG spectra in Figure 1

The SFG spectra were fitted to a series of coherently added Lorentzian shapes[4]

$$I_{\mathrm{SFG}}(\omega_{\mathrm{IR}}) \propto \left| A_{\mathrm{NR}} e^{i\phi} + \sum_{j=1}^{N} \frac{B_j \Gamma_j}{(\omega_{\mathrm{IR}} - \omega_j) + i\Gamma_j} \right|^2 \qquad \text{(S1)}$$

with each vibrational mode j described by amplitude B_j, line width Γ_j and frequency ω_j. The first term accounts for the non-resonant part of the response. Intensity of each vibrational mode is

defined as $I_j \equiv |B_j|^2$. The fitting parameters for Figure 1a in the main text are collected in Table S1.

Table S1. Fitting parameters for the SFG spectra of OA-capped nanoplates on water surface at different coverage rates (see Figure 1a in the main text)

Vibrational mode	Parameters	Fitting results for different coverage rates			
		0.4%	8.3%	25%	100%
CH_2 ss (d^+)	B_1 (a. u.)	0.46	0.62	0.63	0.63
	ω_1 (cm^{-1})	2854	2850	2849	2850
	Γ_1 (cm^{-1})	8.5	12.4	12.3	8.0
CH_3 ss (r^+)	B_2 (a. u.)	0.53	1.07	1.26	1.50
	ω_2(cm^{-1})	2879	2880	2879	2880
	Γ_2 (cm^{-1})	6.0	5.0	6.0	6.0
CH_2 as (d^-)	B_3 (a. u.)	0.25	0.12	0.06	0.05
	ω_3 (cm^{-1})	2906	2906	2907	2906
	Γ_3 (cm^{-1})	8.0	8.0	8.0	6.0
CH_3 Fermi (r^+-FR)	B_4 (a. u.)	0.35	0.70	0.99	1.17
	ω_4(cm^{-1})	2940	2943	2944	2946
	Γ_4 (cm^{-1})	19.0	13.0	10.0	10.0

4. SFG spectra in SPS and PPP polarizations and analysis of methyl orientation angle

SFG spectra were also recorded with SPS and PPP polarization combinations, respectively (Figure S2). An additional peak at ~2970 cm^{-1} was observed at these combinations, which can be assigned to asymmetric stretch of CH_3 (r^-). Moreover, the symmetric stretch of CH_3 and its Fermi resonance mode showed nearly no signal in the SPS configuration. This implies a small average tilt angle of the CH_3 groups.

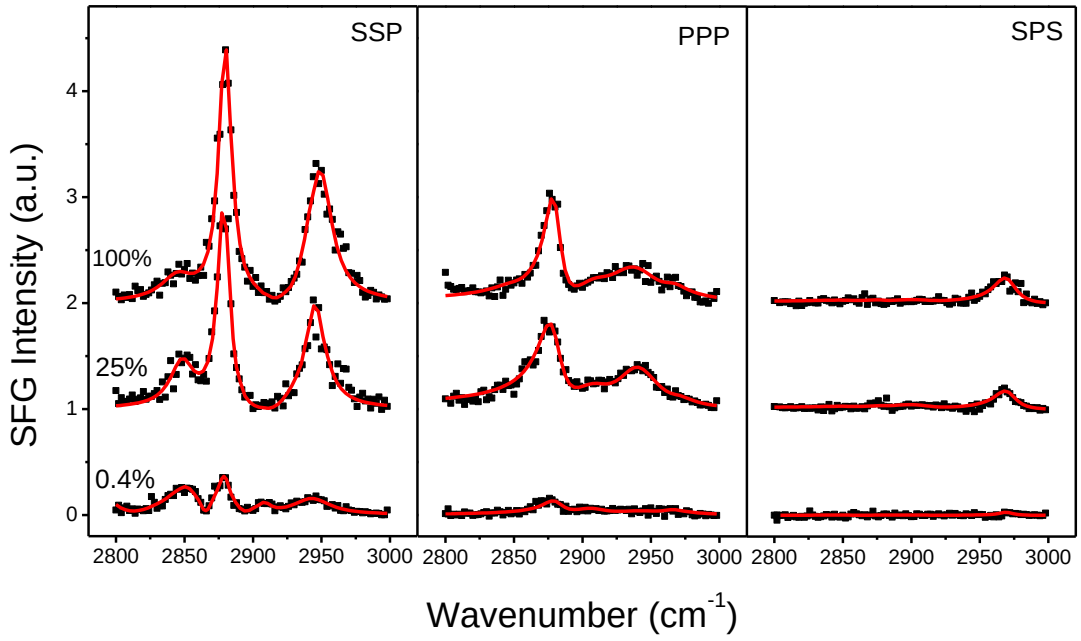

Figure S2. SFG spectra in SSP, PPP and SPS polarization for the OA-capped $NaYF_4$ nanoplates (average side length 40 nm) at different coverage rates on water surface.

The average tilt angle of the terminal methyl groups can be more accurately determined by comparing the r^+ mode intensity in SSP with that in PPP configuration. Methyl group belongs to C_{3v} symmetry, and its title angle (θ) is defined as the angle between its symmetric axis and the

surface normal. The method for analysis θ of CH_3 has been well documented in the literature.[5] By fitting the peaks in Figure S2 to Equation S1, the SSP to PPP intensity ratios at 0.4%, 25%, and 100% surface coverages are found to be 4.6±0.4, 4.1±0.2, and 4.0±0.2, respectively. Accordingly, the CH_3 average tilt angles in the three samples are estimated to be 12.8±3.6°, 6.1±4.4°, and 4.6±4.6°, respectively. Taking into account the relatively large experimental error associated with SFG intensity determination (typically ±5%), it can be concluded that the majority of the terminal methyl groups of OA molecules keep a small tilt angle (close to zero) during the self-assembly of the nanoplates.

5. SFG spectra of nanoplates on CaF_2 substrates

The water-surface-supported nanoplates (40±10 nm) with different surface coverage rates were transferred onto clean CaF_2 window plates separately. After drying of the samples, SFG spectra (Figure S3) were recorded from the air side. The SFG peak positions and the r^+/d^+ order ratios for the transferred nanoplates were somewhat changed comparing to those on water surface. This is normal since CaF_2 substrate is different from water surface in both ligand affinity and refractive index. A noticeable point is that the peak for CH_2 anti-symmetric stretch mode (d^-) was shifted to ~2920 cm^{-1} for non-assembled nanoplates, while for the well-assembled ones we observed a peak at ~2906 cm^{-1} with a shoulder around 2920 cm^{-1}. It is more rational to assign the 2908 cm^{-1} band to a Fermi resonance rather than to anti-symmetric stretch of CH_2. Despite of the above differences, the same fact was observed on either CaF_2 substrates or water surface, i.e. the order ratio of the capping ligands depends on the assembling state of the nanoplates. The higher degree of self-assembly, the larger the order ratio we got. Interestingly, random aggregation of nanoplates does not lead to high order ratio (Figure S3, the triangle-symboled scatter plot), which

can be interpreted by that the SFG resonance of the methyl groups is heavily cancelled out because of their arbitrary orientations in the aggregates.

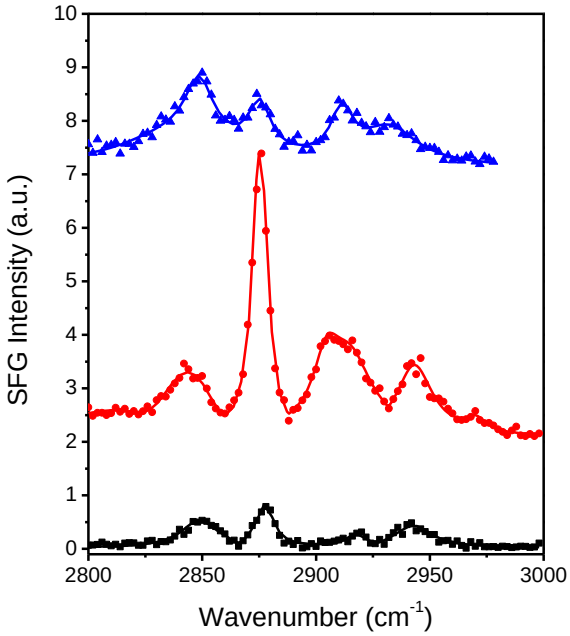

Figure S3. SFG spectra (SSP) of oleic acid-capped nanoplates on CaF_2 substrates, offset for a clear view. The coverage rates of the nanoplates on water surface before transferring were ~0.4% (black squares) and ~100% (red circles), respectively. For comparison, SFG spectrum was also recorded for randomly aggregated nanoplates (blue triangles), which were prepared by drop-casting a certain amount of the stock solution of nanoplates (in chloroform) directly onto CaF_2 substrates. The order ratios (r^+/d^+) for the three samples are 1.5 (non-assembled state), 4.1 (assembled state) and 0.8 (randomly aggregated state), respectively.

6. Estimation of "additional" free volume

If the capping ligands on the top facet were all-trans and the molecular long axes were uniformly oriented along the normal direction of the underlying surface, the total space they

occupy would be a hexagonal column. The base of the column equals to the facet and the height is the ligand chain length (L). The volume of the column is thus given by $V = \frac{3\sqrt{3}}{2}a^2L$, where a is the side length of the hexagonal facet. The outwards lying down of the edge ligands will provides more available room in addition to the columnar space. For each of the six edges, the additional free volume can be mathematically divided into two parts as shown in Figure S4. One part is a quarter of a circle cylinder with a base radius of L and a height of a. The other part is one six of a semisphere with a radius of L.

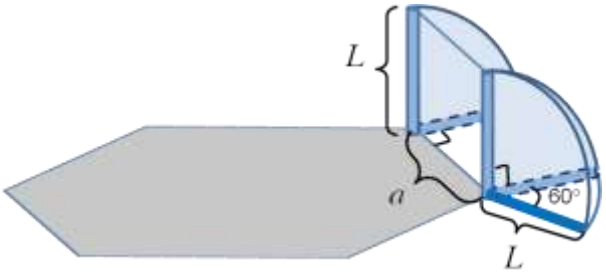

Figure S4. Schematic representation of the additional free volume brought by the facet edge.

The additional free volume provided by the six facet edges in total:

$$\Delta V = 6 \times \frac{\pi}{4}L^2a + \frac{2\pi}{3}L^3 \qquad \text{(S1)}$$

Let $x = L/a$, the ratio of the additional volume to the hexagonal columnar volume can be formulated as:

$$\frac{\Delta V}{V} = \frac{6 \times \frac{\pi}{4}L^2a + \frac{2\pi}{3}L^3}{\frac{3\sqrt{3}}{2}a^2L} = \frac{\sqrt{3}}{3}\pi x + \frac{4\sqrt{3}}{27}\pi x^2 \approx 1.8x + 0.8x^2 \qquad \text{(S2)}$$

7. SFG results for OA Langmuir monolayer

In the main text we assume a high capping density of OA on the nanoplates. To confirm this assumption, we compare the SFG data for OA on nanoplates with that obtained for OA molecules on water surface. OA is a typical amphiphilic molecule that can form Langmuir monolayer on water. In a previous report, SFG spectra of OA monolayers have been analyzed in combination with surface pressure–molecular area isotherm.[6] As expected, conformational ordering of OA was observed with decreasing molecular area (increasing packing density). However, when calculating the order ratio (r^+/d^+) base on the figure therein (Fig.3 in ref. 6), we find that even for the most compressed OA monolayer with a molecular area of 0.25 nm^2, the order ratio is only about 1.6. Our own measurements also show that the maximum order ratio for OA monolayer on water surface is less than 2.1 (Figure S5), much lower than that achieved on the well-assembled nanoplates (Figure 1 in the main text). Furthermore, the overall SFG intensity of the OA Langmuir monolayer is found to be one order magnitude lower than that obtained on the assembled nanoplates under the same measuring conditions. These facts strongly suggest that the surface density of OA molecules on the nanoplates (the top facets) is higher than that in the densest Langmuir monolayer (4×10^{14} molecules cm^{-2}). This is in coincidence with our assumption and can be explained by the relative small size of the non-solvated head groups and the strong binding interaction with the underlying surface in the former case.

Experimental details for Figure S5 and discussions: Oleic acid (OA) was dissolved in chloroform at a proper concentration and a series of different amounts of this solution were drop-cast onto water surface separately. The same container and the same amount of water (Mili-Q) were used for preparing each sample. In principle, when more amount of OA is dropped, the surface density of OA will increase until the total amount exceeds that needed for full monolayer

coverage. The maximum achievable surface density depends on the size of the head group. One would expect a conformational and orientational ordering of the hydrophobic tails with increasing surface density. The SFG order ratio (CH_3 to CH_2 stretch mode) of OA molecules should also increase correspondingly, and reach a plateau at full monolayer coverage. Our SFG results agree with the above expectation. The maximum order ratio for OA Langmuir monolayer is ~2.0, substantially lower than that obtained for OA on assembled $NaYF_4$ nanoplates.

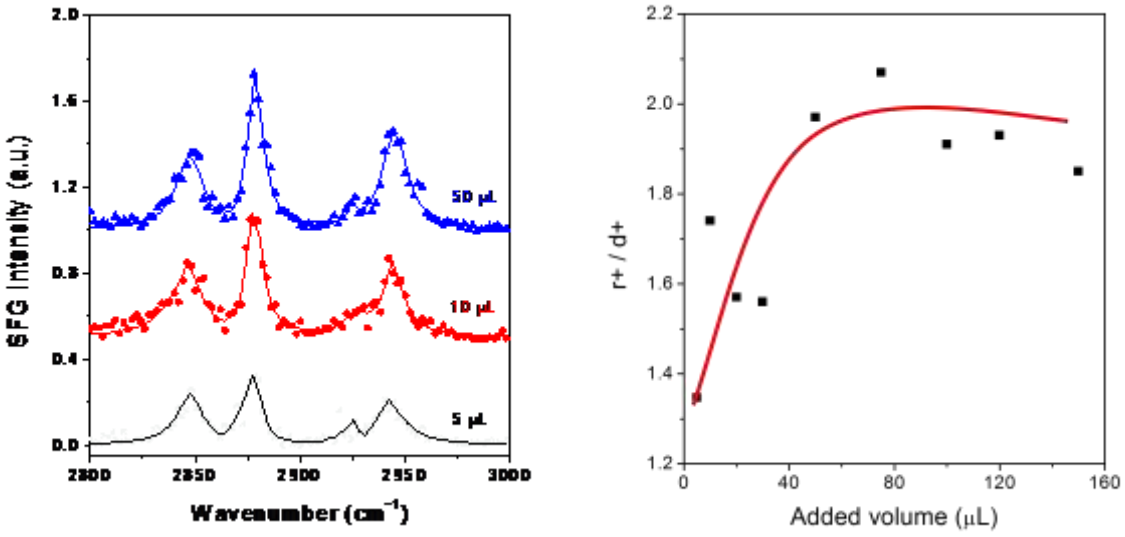

Figure S5. Left: SFG spectra (SSP) of OA Langmuir monolayer films with different surface densities on water. Right: order ratio as a function of added amount of the OA stock solution.

References:

(1) Wang, L. Y.; Li, Y. D. Controlled Synthesis and Luminescence of Lanthanide Doped $NaYF_4$ Nanocrystals. *Chem. Mater.* **2007,** *19*, 727-734.

(2) Zeng, S. J.; Ren, G. Z.; Xu, C. F.; Yang, Q. B. High Uniformity and Monodispersity of Sodium Rare-Earth Fluoride Nanocrystals: Controllable Synthesis, Shape Evolution and Optical Properties. *Crystengcomm* **2011,** *13*, 1384-1390.

(3) Ye, X. C.; Collins, J. E.; Kang, Y. J.; Chen, J.; Chen, D. T. N.; Yodh, A. G.; Murray, C. B. Morphologically Controlled Synthesis of Colloidal Upconversion Nanophosphors and Their Shape-Directed Self-Assembly. *Proc. Nat. Acad. Sci. U. S. A.* **2010,** *107*, 22430-22435.

(4) Weeraman, C.; Yatawara, A. K.; Bordenyuk, A. N.; Benderskii, A. V. Effect of Nanoscale Geometry on Molecular Conformation: Vibrational Sum-Frequency Generation of Alkanethiols on Gold Nanoparticles. *J. Am. Chem. Soc.* **2006,** *128*, 14244-14245.

(5) Zhuang, X.; Miranda, P. B.; Kim, D.; Shen, Y. R. Mapping Molecular Orientation and Conformation at Interfaces by Surface Nonlinear Optics. *Phys. Rev. B* **1999,** *59*, 12632-12640.

(6) Kleber, J.; Lass, K.; Friedrichs, G. Quantitative Time-Resolved Vibrational Sum Frequency Generation Spectroscopy as a Tool for Thin Film Kinetic Studies: New Insights into Oleic Acid Monolayer Oxidation. *J. Phys. Chem. A* **2013,** *117*, 7863-7875.